The Supporting Information

Chiral Sensing Combined with Nuclease Activity Assay to Track Cas9 Dynamics in Solution: ROA and CPL study

Monika Halat[1]*, Magdalena Klimek-Chodacka[1], Agnieszka Domagała[2,3], Grzegorz Zając[2], Tomasz Oleszkiewicz[1], Josef Kapitan[4] and Rafal Baranski[1]

[1] Department of Plant Biology and Biotechnology, Faculty of Biotechnology and Horticulture, University of Agriculture in Krakow, AL. Mickiewicza 21, 31-120 Krakow, Poland; m.halat@urk.edu.pl;
[2] Jagiellonian Centre for Experimental Therapeutics (JCET), Bobrzynskiego 14, 30-348 Krakow, Poland
[3] Doctoral School of Exact and Natural Sciences, Jagiellonian University, Prof. S. Łojasiewicza 11, 30-348 Krakow, Poland
[4] Department of Optics, Palacký University Olomouc, 17. listopadu 12, 77146, Olomouc, Czech Republic
* Correspondence to: m.halat@urk.edu.pl

Table of contents

1. Materials and Methods

1.1 Eu(III)-based probes

Detailed synthesis protocols of the NaEuEDTA and $Na_3[Eu(DPA)_3]$ complexes were described previously.[1] Eu(III)-probes stock solutions were prepared by dissolving each in the certificate nuclease-free water (Integrated DNA Technologies Inc., IDT) to the final concentration of 40 mM.

2.2 SpyCas9 protein and filtrate

The SpyCas9 protein, in detail Alt-R™ S.p. Cas9 V3, glycerol-free containing nuclear localization sequence (NLS) and C-terminal 6-His tag (cat. no. 10007807), was purchased from IDT (Leuven, Belgium), as a ready-made solution without glycerol, with a nuclease concentration of 10 mg/ml (61 µM), and in this form, the protein sample was used for ROA measurement. For the ROA-CPL study, the commercial SpyCas9 solution was diluted to 1 mg/ml (6.1 µM) using 1X PBS buffer in nuclease-free water (IDT). Then, a Eu(III)-based probe, $EuEDTA^-$ or $[Eu(DPA)_3]^{3-}$, was added to get the final probe concentration of 2 mM.
Due to company policy, the exact composition of the SpyCas9 buffer solution is unknown. Therefore, the commercial PBS buffer was filtered through an Amikon 100 kDa protein filter (Merck) to measure the ROA of the filtrate and determine how the buffer composition affected spectra of Eu(III) treated SpyCas9.

2.3 gRNA design and transcription

The 20 nt gRNA was designed to target the second exon in the flavanone-3-hydroxylase (*F3H*) carrot (*Daucus carota* L.) gene (NCBI Acc. No. AF184270.1) at 632–651 position (GAAGTTTTGTCAGAGGCCAT) using the CasOT software. The complementary DNA oligonucleotide was synthesized, assembled with the tracrRNA, and verified as described previously. [2,3]
ROA measurements were performed using an aqueous solution of gRNA at the concentration of 9 µg/µl (264 µM). In turn, ROA-CPL measurements were carried out using a diluted solution of gRNA (6.1 µM) with nuclease-free water (IDT) enriched with the proper Eu(III) probe (the final Eu(III) probe concentration was 2 mM).

2.4 RNP complex preparation

To form a catalytically active ribonucleoprotein (RNP) complex, the synthesized gRNA was added to the SpyCas9 solution maintaining a 1:1 molar ratio (1830 pmol of the SpyCas9 in 30 µl mixed with 1830 pmol of gRNA in 7 µl). Then, the RNP solution (8.1 mg/ml; 49.41 µM) was incubated at 25°C for 20 min. In the case of the ROA-CPL measurements, the RNP sample (1 µg/µl; 6.1 µM) was additionally enriched with an appropriate Eu(III)-probe solution to get a 2 mM final concentration of the probe.

2.5 ROA and CPL measurements

Sample Preparation

All samples (**Table S1**) were measured in ROA quartz cuvettes (100 µl volume) with antireflecting coating, with no further sample preparation. Stable temperature conditions of 20°C during the measurement, were kept using the ROA temperature cell compartment.

Instrumentation

All presented here Raman, ROA, total luminescence (TL), and CPL spectra were recorded simultaneously using the Chiral*RAMAN-2X*™ spectrometer from BioTool Inc., equipped with the back-scattering geometry, the scattered circular polarization (SCP) modulation scheme, and the green Nd:YAG laser with an excitation wavelength of 532 nm. The instrument collected spectra in the range from 100 to 2500 cm^{-1} with a spectral resolution of 7 cm^{-1}. The incident laser power and the integration time were set individually for each sample. All measurement parameters are shown in **Table S1**. Raman spectra for the solvents were also recorded keeping the same measurement parameters (laser power, integration time, temperature), as well as the same type and orientation of the ROA cuvette.

Table S1. Individual ROA measurement parameters dictated by the type of sample and its concentrations.

	ROA/CPL parameters		
Type of sample	Laser power	Integration time	Accumulation time
SpyCas9 protein (61 µM)	750 mW	4.022 s	48 h
RNP complex (49.45 µM)	865 mW		
gRNA (264 µM)	660 mW		
$[Eu(DPA)_3]^{3-}$ (2 mM)	60 mW	2.058 s	24 h
$EuEDTA^-$ (2 mM)	550 mW		
SpyCas9 (6.1 µM) + $[Eu(DPA)_3]^{3-}$ (2 mM)	70 mW		
RNP (6.1 µM) + $[Eu(DPA)_3]^{3-}$ (2 mM)			
gRNA (6.1 µM) + $[Eu(DPA)_3]^{3-}$ (2 mM)	80 mW		
SpyCas9 (6.1 µM) + $EuEDTA^-$ (2 mM)	350 mW		
RNP (6.1 µM) + $EuEDTA^-$ (2 mM)			
gRNA (6.1 µM) + $EuEDTA^-$ (2 mM)	360 mW		

Data processing

Overall structure of the SpyCas9 protein (PDB ID: 4CMP)[4] and its catalytic active RNP complex (PDB ID: 4ZT0)[5] were presented in ribbon representation using PyMOL software.
Raw Raman and ROA spectra were further processed in *Origin Pro* software by solvent spectra subtraction and baseline correction. In addition, each ROA dataset was smoothed with the FFT filter method by 3 points of window or with the Savitzky Golay method (Raman-TL and ROA-CPL spectra) by individually set points of window.

2.6 Nuclease activity assay

DNA amplification and in vitro cleave

DNA amplification was conducted as previously described.[3] Two primers (F: 5'-GCAAGATTGGCGAGAGATAG-3' and R: 5'-AGCAAGAGCGTAATTGTGCC-3') were designed to amplify a 309 bp DNA fragment of the *F3H* carrot gene (NCBI Acc. No. AF184270.1) comprising the gRNA target site. The F primer was labelled with the FAM fluorescent dye at its 5' end. The RNP nuclease activity was assessed by calculating the ratio of fluorescently labelled cleaved products to uncleaved amplicons after detecting labelled DNA using capillary electrophoresis (3730XL DNA Analyzer, Applied Biosystems, Foster City, CA, USA). Both the SpyCas9 protein and the RNP complex were verified for nucleolytic activity before and after ROA and CPL measurements.

DNA cleavage in living cells (in vivo)

Protoplasts were isolated from cells of callus (line No. 10F), derived from the Koral carrot cultivar, and maintained in vitro according to a previously described protocol.[6] Isolated protoplasts were incubated in W5 solution (154 mM NaCl; 125 mM $CaCl_2$; 5 mM KCl; 5 mM glucose; pH 5.6)[7] on ice for one hour, then centrifuged (145rcf for 5 min.) and resuspended in the MMG solution (4 mM MES, 0.4 M mannitol, 15 mM $MgCl_2$, pH 5.7) at the concentration of 1×10^6 protoplasts per ml. 300 µl of suspended protoplasts was transferred into a culture tube and 20 µl of suspension containing 10 µg of RNPs followed by 320 µl PEG solution (40% w/v PEG4000, 0.2 M mannitol, 100 mM $CaCl_2$ $2H_2O$) were added and instantly mixed by a gently tapping the tube. Protoplasts were then incubated for 10 min. at room temperature. After incubation, 5 ml of W5 solution (room temperature) was added, mixed by inverting a tube and centrifuged (145 rcf for 5 min.). Supernatant was gently removed using a Pasteur pipette, protoplasts were resuspended in 8 ml of the CPP protoplast culture medium[8] and centrifuged (145 rcf for 5 min.). Supernatant was removed again and protoplasts were resuspended in 300 µl of the CPP medium. Protoplasts were incubated at 26°C, in the dark. After 72 h, protoplasts were transferred to 2 ml tube, centrifuged, the medium was discarded and protoplasts were frozen and kept at -20°C, until DNA isolation for PCR amplification.

2. Results

2.1. Nuclease activity assays

DNA cleavage assay for concentrated SpyCas9 and RNP

PCR amplification of the target DNA site for Cas9, complementary to the gRNA, produced the expected 309 bp fragments. To verify the nucleolytic activity of RNP complexes post-ROA measurement, 309 bp DNA fragments were incubated with RNP samples. Two DNA fractions were observed: intact 309 bp DNA and a cleaved fraction of 150–162 bp (**Fig. S1**). The same cleavage products were obtained in our previous experiments.[3] Cleaved products constituted 83.3% in the control (non-measured) sample and 79.3–80.8% in the measured samples, based on fluorescent signal area analysis of labelled DNA fragments. No cleavage was detected in the RNP-free control.

DNA cleavage assay for diluted SpyCas9 and RNP enriched with Eu(III)-probes

The activity assay was repeated with SpyCas9 and RNP samples treated with either $EuEDTA^-$ or $[Eu(DPA)_3]^{3-}$. Cleaved DNA percentages were similar in non-measured (95.3%) and CPL/ROA-measured (94.9%) samples (**Table S2**), with the paired t-test indicating no significant difference (12 samples, $p = 0.467$). To assess whether CPL measurement affects RNP complex stability, samples were supplemented with additional gRNA. Supplemented samples showed slightly increased activity (96.1%) compared to non-supplemented ones (93.4%), though the difference was not statistically significant (8 samples, $p = 0.134$). A minor difference in activity was noted between samples treated with $EuEDTA^-$ (93.9%) and EuDPA (96.3%), with the difference approaching the significance threshold (12 samples, $p = 0.051$). The *in vitro* cleavage assays confirmed that the RNPs used in CPL/ROA measurements had high nucleolytic activity, which remained consistent post-measurement. The addition of Eu(III)-probes to enhance CPL signals did not significantly affect SpyCas9 or gRNA:SpyCas9 complex activity. However, $[Eu(DPA)_3]^{3-}$ appeared to interfere less with RNP activity compared to $EuEDTA^-$.

RNP activity assay in living cells

The RNP activity post-CPL/ROA measurement was also assessed in a biological system using isolated carrot protoplasts, which are suitable for gRNA:SpyCas9 RNP complexes delivery and cleavage activity assessment, as previously reported.[9] Polyethylene glycol (PEG)-mediated delivery of RNP complexes into living protoplasts was conducted, and DNA was isolated after 72 hours. Sequencing revealed mutations at the gRNA target site (**Fig. S2**). These mutations were single-nucleotide insertions, occurring 3 nt upstream of the PAM sequence, as expected. No mutations were detected in control protoplasts treated with PEG alone.

Table S2. SpyCas9 and gRNA:SpyCas9 ribonucleoprotein (RNP) complex activity pre- and post-CPL/ROA measurements, expressed as the percentage of cleaved DNA fragments.

Sample *	**% of cleaved DNA in**	
	pre-measurement sample	post-measurement sample
Control (309 bp DNA only)	0	n.d.
RNP (control)	96.0	n.d.
Cas9-EuEDTA**	95.2	95.6
RNP-EuEDTA	92.3	89.3
RNP-EuEDTA +extra gRNA	95.2	95.9
Cas9-EuDPA**	96.3	96.3
RNP-EuDPA	96.1	95.7
RNP-EuDPA +extra gRNA	96.8	96.6

* 309 bp DNA fragments were added to each sample

** After CPL measurement, Cas9 was incubated with gRNA to form the RNP complex for the nucleolytic activity assay.

n.d. - not determined

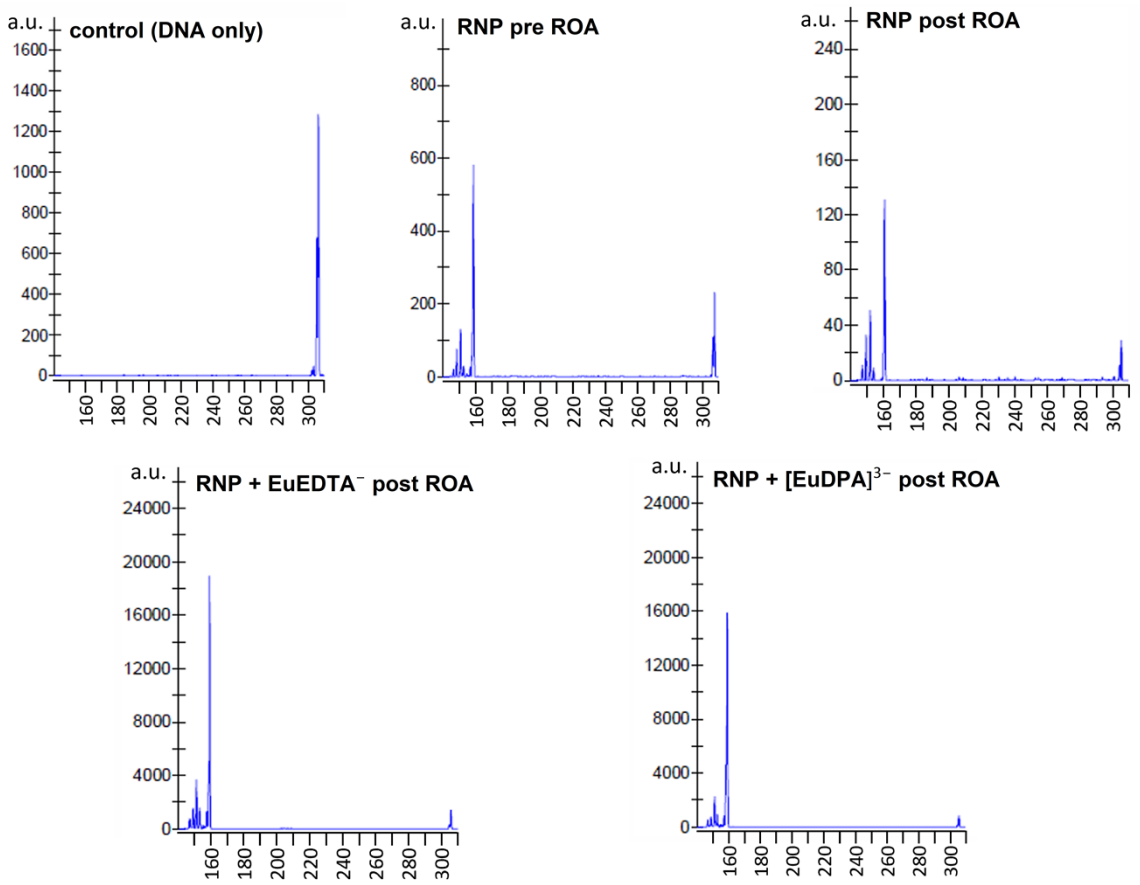

Fig. S1. Electropherograms of ROX-labelled DNA fragments detected by capillary electrophoresis. Samples include: DNA only, RNP pre-ROA, RNP post-ROA, RNP treated with EuEDTA post-ROA, and RNP treated with EuDPA post-ROA. The 150–162 bp DNA fragments are products of RNP-mediated cleavage of 309 bp DNA fragments (a.u. = arbitrary units).

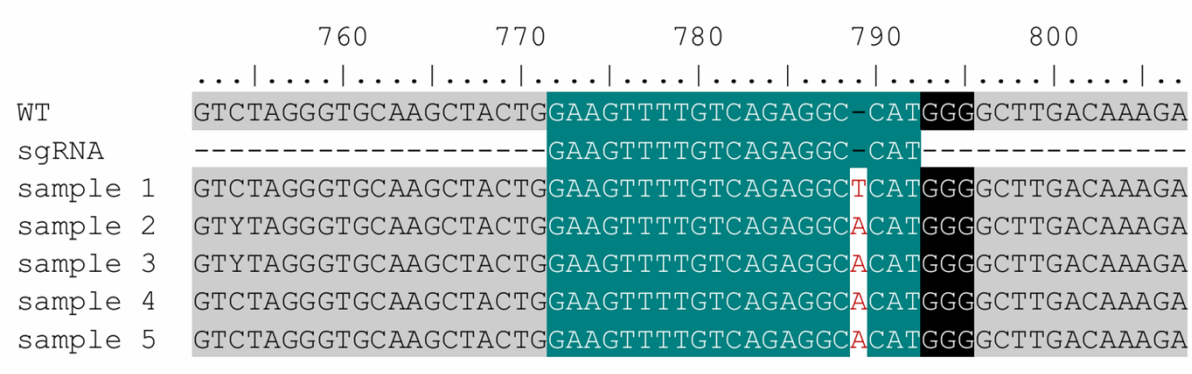

Fig. S2. DNA sequences at the gRNA target site. WT: wild-type DNA from PEG-treated protoplasts. Samples 1–5: DNA from protoplasts after PEG-mediated delivery of RNPs post-ROA. sgRNA: single-guide RNA. PAM sequence is highlighted in black, and single-nucleotide insertions (adenine or thymine) are marked in red.

2.2 Analysis and origin of bands in Raman and ROA spectra

Raman spectra of SpyCas9 protein and its RNP complex

Raman spectra of SpyCas9 (blue) and RNP (red) samples are shown in **Fig. S3**. These spectra correspond to the ROA spectra shown in **Fig. 2** of the manuscript and were collected simultaneously during 48 h of Raman/ROA accumulation. Both Raman profiles show similar spectral features, with the most intense bands occurring at 883, 995 and 1082 cm^{-1} and can also be observed in the Raman spectrum of protein filtrate (**Fig. S3,** dark grey). These significant Raman bands can be attributed to the orthophosphate H_3PO_4 (>600 mM) buffered at pH ~6, in detail to: the hydrogen-bonding phosphate H atoms, the symmetric stretch that appears when the phosphate is deprotonated ($H_2PO_4^-$, HPO_4^{2-}), and to the asymmetric stretch of the same groups, respectively.[10] The remaining bands of the filtrate are also of inorganic origin and can be assigned to the symmetric (395 cm^{-1}) and asymmetric (530 cm^{-1}) bending vibrations of the PO_4^{3-} group.[11] The 1124-1760 cm^{-1} spectral range, highlighted and magnified in a black box, reveals bands connected with protein secondary structure that are invisible in the filtrate spectrum[12] (**Table S3**). Comparing those bands there is no significant difference indicating serious changes in the α-helical conformation of the SpyCas9. Upon gRNA binding, two new bands arise from the red profile (1576, 1281 cm^{-1}) suggesting a slight change in the geometry of aromatic residues (Tyr, tyrosine; Trp, tryptophan; Phe, phenylalanine). An increase in the intensity of the 1456 cm^{-1} band resulting from the C-H deformation is also visible, which may indicate a change in the orientation of the side chains in the α and β elements. There are no Raman bands typical for nucleic acids in the RNP spectrum (**Table S3**). In summary, the Raman spectra of SpyCas9 nuclease and its active RNP complex are dominated by the bands of the filtrate with a possible inorganic phosphate buffer composition. Some low-intensity protein bands are visible, however, this is not sufficient to identify important structural changes due to gRNA association. In shows, ROA spectroscopy is more sensitive to detect rearrangements in the SpyCas9 geometry (**Fig. 2** of the manuscript).

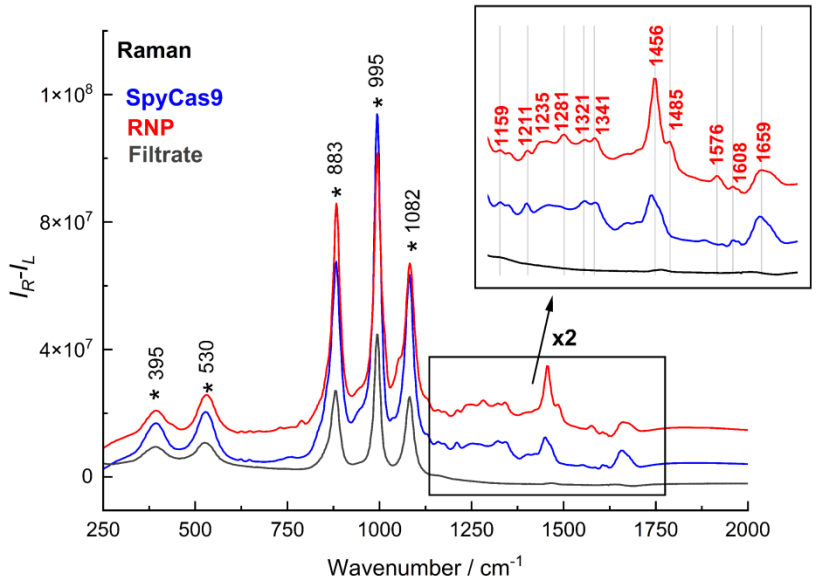

Fig. S3. Raman spectra of SpyCas9 nuclease (blue), RNP complex (red), and SpyCas9 filtrate (dark gray) recorded under similar conditions and pre-processed in Origin Pro software with baseline correction and water subtraction. The area marked in the box has been enlarged twice. Raman bands marked by the asterisk are assigned to the filtrate.

Table S3. Assignments of Raman bands for SpyCas9, RNP and filtrate (*).[10–12]

Wavenumber [cm^{-1}]	Assignments	Secondary structure
1659	Amide I C=O streching	α-helix
1608	aromatic residues Tyr, Trp, Phe	α-helix
1576	indole ring (Trp)	β-sheet
1456/1485	C-H deformations	α/β-elements
1341/1321	Cα–H deformations (Trp)	α-helix
1281/1230/1211	Amide III coupled C–N stretching and N–H bending	α/β-elements
1159	C–N streching	α-helix
1082*	$H_2PO_4^-$, HPO_4^{2-}asymmetric stretching	none
995*	$H_2PO_4^-$, HPO_4^{2-}symmetric stretching	
883*	hydrogen-bonding phosphate H atoms	
530*	PO_4^{3-} symmetric bending	
396*	PO_4^{3-} asymmetric bending	

ROA accumulation of SpyCas9 filtrate

To confirm that the SpyCas9 protein is the only chiral component of the commercial nuclease solution, we performed ROA measurements of the residual solvent after the protein standard filtration. Therefore, we kept the same parameters as we used for the SpyCas9 nuclease and its RNP complex (4 s of acquisition time, 750/865 mW of laser power, 48 h of accumulation). **Fig. S4** shows the obtained ROA spectra, practically only noise, which indicates the absence of chiral compounds in the filtrate solution or possibly their very low concentrations. However, the experimental ROA spectra of macromolecules being studied are affected by filtrate Raman bands ('*', Fig. 2 in the manuscript). These Raman bands (below 1130 cm^{-1}) may leak into the ROA spectra due to polarization artifacts, incorrect signal compensation, or detector saturation during the measurements. However, artifacts did not penetrate the most sensitive regions of the ROA spectrum, such as the amide I and amide III range, which allowed the detection and interpretation of changes in the SpyCas9 protein geometry upon gRNA binding.

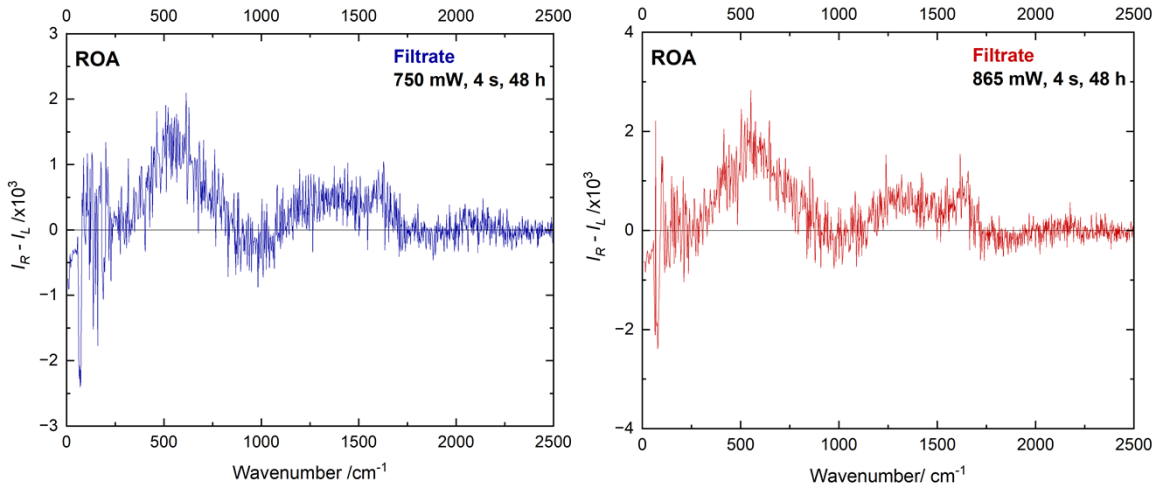

Fig. S4. ROA spectra of SpyCas9 filtrate registered after 48 hours with 4s of acquisition time, 750 mW (dark blue) and 865 mW (red) laser power.

Raman and ROA spectra of gRNA

The Raman (black) and ROA (cyan) spectra of the gRNA solution used in the RNP complex formation are presented in **Fig. S5**. In general, ROA spectroscopy is sensitive to four sources of nucleic acid chirality: the chiral stacking arrangement of non-chiral base rings, the chiral orientation of the base and sugar rings in relation to the C–N glycosidic bond, the molecular chirality originating from the asymmetric centres of sugar rings and the chiral conformation of the sugar–phosphate backbone. Three major spectral regions can be distinguished in nucleic acid ROA spectra: 1/ ~900 – 1150 cm^{-1} associated with vibrations of the sugar rings and phosphate backbone; 2/ ~1200 – 1550 cm^{-1} dominated by sugar-base modes that reflect the mutual rings disposition and the sugar ring conformation; 3/ ~1550 – 1750 cm^{-1} consisted of ROA patterns typical for the type of the base-stacking arrangement. One of the best described ROA features for RNA such as the intensive –/+/– triplet of the sugar-phosphate range is observed at 992, 1055, and 1094 cm^{-1}, respectively, as well as it has been assigned to A-type double helical polyribonucleotide where the sugar puckers are mainly C3′-*endo*.[13,14] Assignment of the rest ROA bands is challenging due to limited studies of nucleic acids in scientific literature and very rare theoretical simulations.[15] The origin of some Raman bands is defined in the **Table S4**.

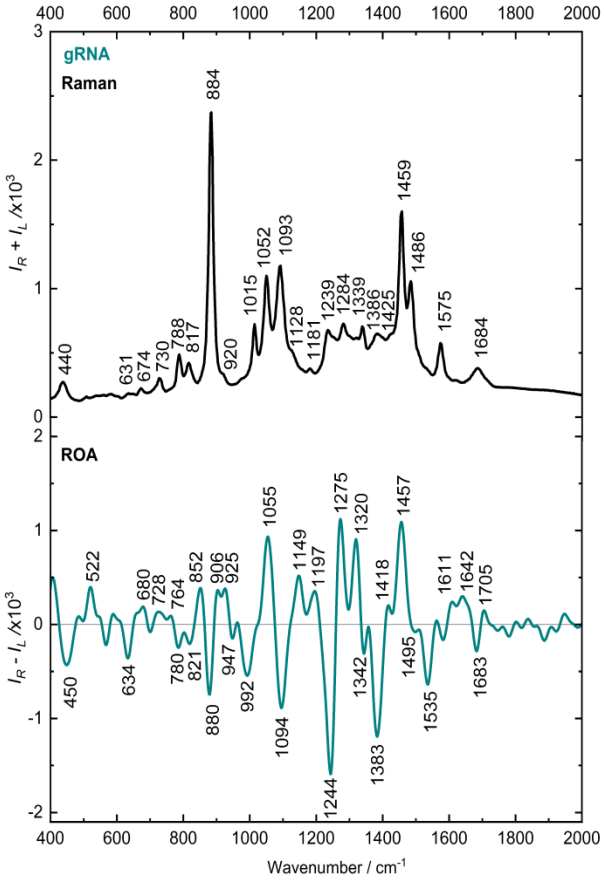

Fig. S5. Raman (black) and ROA (cyan) spectra of gRNA nuclease-free water solution (9 mg/ml; 264 µM). Baseline subtraction using and smoothing based on the FFT filter function and 7 windows points were provided in Origin software.

Table S4. Assignments of Raman and ROA bands for gRNA in nuclease-free water solution (9 mg/ml; 264 µM).[14,16]

Wavenumber [cm^{-1}]		Assignment
RAMAN	**ROA**	
440	+406 –450	G out of plane ring deformations
631	–634	A/U/G/C
674	+660	G out of plane ring deformations
730	+733	A ring stretching
788	+764 –760	C/U breathing/stretching
817	+821	O–P–O symmetric stretching, marker for A-form helix
884	+852 –880 +906	A/U/G/C out of plane ring deformations, backbone Ribose–phosphate
920	+925 –947	Ribose–phosphate, –C–O– stretching
1015 1052 1093	–992 +1055 –1094	P–O stretch, sugar phosphate –C–O– stretching PO 2 symmetric stretching ROA triplet: A-form RNA
1128	-	Stretching at 2’ position of ribose
1181	+1149	A/U/G/C ring; external C–N stretching
1239	–1244	U/C ring stretching
1284	+1275	A/G ring stretching
1339	+1320	A/G/U
1386	–1342 –1383	A/G/U
1425	+1418	A/G ring stretching, CH deformations
1459	+1457	U/C ring stretching, CH deformations
1486	–1495	A/G ring stretching/planar vibrations
1575	–1535	A/G ring stretching
1684	+1642 –1683 +1705	C=O stretching, N-H bending T/G/C ROA couplet; right-handed helix

Comparison of CID values for CPL bands

Table S5. Comparison of CID values ($(I_R - I_L)/(I_R + I_L)$ ratio) calculated for CPL bands of $[Eu(DPA)_3]^{3-}$ and $EuEDTA^-$ assigned to the $^5D_0 \rightarrow {}^7F_1$ electronic transition of Eu(III).

	$[Eu(DPA)_3]^{3-}$			**$EuEDTA^-$**		
	$^5D_0 \rightarrow {}^7F_1$			**$^5D_0 \rightarrow {}^7F_1$**		
	cm^{-1}	*nm*	*CID*	*cm^{-1}*	*nm*	*CID*
SpyCas9	1862	590	-7.26×10^{-5}	1854	590	-2.16×10^{-5}
	1978	595	-1.23×10^{-4}	2012	596	5.64×10^{-5}
gRNA	1837	590	8.64×10^{-6}	1919	592	6.79×10^{-5}
	1987	595	1.69×10^{-5}			
RNP	1843	590	7.09×10^{-6}	1830	589	-1.64×10^{-5}
	1933	593	8.65×10^{-6}	1914	592	1.95×10^{-4}
	1998	595	1.88×10^{-5}	1977	595	-4.61×10^{-5}
	2060	597	2.80×10^{-5}	2056	597	1.42×10^{-4}
				2092	599	2.35×10^{-4}

3. References:

1 A. Domagała, S. Buda, M. Baranska and G. Zając, *Spectrochim Acta A Mol Biomol Spectrosc*, 2025, **324**, 124995.
2 M. Klimek-Chodacka, T. Oleszkiewicz, L. G. Lowder, Y. Qi and R. Baranski, *Plant Cell Rep*, 2018, **37**, 575–586.
3 M. Halat, M. Klimek-Chodacka, J. Orleanska, M. Baranska and R. Baranski, *Int J Mol Sci*, 2021, **22**, 1–14.
4 M. Jinek, F. Jiang, D. W. Taylor, S. H. Sternberg, E. Kaya, E. Ma, C. Anders, M. Hauer, K. Zhou, S. Lin, M. Kaplan, A. T. Iavarone, E. Charpentier, E. Nogales and J. A. Doudna, *Science (1979)*, 2014, **343**, 1247997.
5 F. Jiang, K. Zhou, L. Ma, S. Gressel and J. A. Doudna, *Science (1979)*, 2015, **348**, 1477–1481.
6 E. Grzebelus, M. Szklarczyk and R. Baranski, *Plant Cell, Tissue and Organ Culture (PCTOC)*, 2012, **109**, 101–109.
7 L. Menczel, F. Nagy, Z. R. Kiss and P. Maliga, *Streptomycin Resistant and Sensitive Somatic Hybrids of Nicotiana tabacum + Nicotiana knightiana: Correlation of Resistance to N. tabacum Plastids*, 1981, vol. 59.
8 R. Dirks, V. Sidorov and C. Tulmans, *Theoretical and Applied Genetics*, 1996, **93**, 809–815.
9 M. Klimek-Chodacka, M. Gieniec and R. Baranski, *Int J Mol Sci*, DOI:10.3390/ijms221910740.
10 L. P. Heighton, M. Zimmerman, C. P. Rice, E. E. Codling, J. A. Tossell, W. F. Schmidt, L. P. Heighton, M. Zimmerman, C. P. Rice, E. E. Codling, J. A. Tossell and W. F. Schmidt, *Open Journal of Soil Science*, 2012, **02**, 55–63.
11 M. Kazanci, P. Fratzl, K. Klaushofer and E. P. Paschalis, *Calcif Tissue Int*, 2006, **79**, 354–359.
12 A. Rygula, K. Majzner, K. M. Marzec, A. Kaczor, M. Pilarczyk and M. Baranska, *Journal of Raman Spectroscopy*, 2013, **44**, 1061–1076.
13 E. W. Blanch, L. Hecht and L. D. Barron, *Methods*, 2003, **29**, 196–209.
14 A. J. Hobro, M. Rouhi, E. W. Blanch and G. L. Conn, *Nucleic Acids Res*, 2007, **35**, 1169–1177.
15 M. Krupová, J. Kessler and P. Bouř, *Chempluschem*, 2020, **85**, 561–575.
16 M. Gąsior-Głogowska, K. Malek, G. Zajac and M. Baranska, *Analyst*, 2016, **141**, 291–296.